Partial Shading Analysis of Multi-String PV Arrays and Derivation of Simplified MPP Expressions

Georgios N. Psarros, *Student Member, IEEE*, Efstratios I. Batzelis, *Student Member, IEEE*, and Stavros A. Papathanassiou, *Senior Member, IEEE*

***Abstract*--In this paper, the electrical response of a partially shaded photovoltaic (PV) array, comprising several strings connected in parallel, is investigated. The PV array is simulated by employing an enhanced version of the widely used single-diode model, reformulated in an explicit manner employing the Lambert W function. The multiple maximum power points (MPPs) that appear on the *P-V* characteristic of the array in partial shading conditions are analyzed, in terms of their number and properties. Simplified empirical expressions are then derived to calculate the voltage, current and power for each local MPP, at any irradiance level and temperature, using only datasheet information, in a most simple and straightforward manner, without resorting to detailed modeling and simulations. The derived formulae are validated using both simulation and experimental results.**

***Index Terms*-Direct expressions, energy model, explicit, local maxima, maximum power point (MPP), partial shading, photovoltaic (PV) array, power peaks, simplified expressions.**

NOMENCLATURE

a	Modified diode ideality factor of the PV cell.
a_{bp}	Modified diode ideality factor of the bypass diode.
α_{Imp},α_{Isc}	Temperature coefficients of I_{mp} and I_{sc}.
b	Breakdown correction factor of the PV cell.
G_j^i	Irradiance incident on cell string group j of PV string i, in per unit (p.u.) of the STC value (1000 W/m^2).
I_{mpj}^i	PV string i current at MPP_j^i.
I_{mpAj}^i	PV array current at $MPPA_j^i$.
I_{mpB}	PV array current at *MPPB*.
I_{ph}	PV cell photocurrent.
$I_{SC,cs}$	PV cell string short circuit current.
I_s	PV cell diode saturation current.
I_{sbp}	Bypass diode saturation current.
MPP_j^i	Local maximum power point j of PV string i.
$MPPA_j^i$	Local maximum power point A of the PV array correlated to MPP_j^i of PV string i.
$MPPB$	Local maximum power point B of the PV array.
m	Breakdown coefficient of the PV cell.
N_j^i	Number of cell strings in group j of string i.
N_{cs}	Number of series-connected cell strings within each PV module.
N_m	Number of PV modules in the PV string.
N_p	Number of parallel connected strings in the PV array.
N_s	Number of series-connected cells in a cell string.
n_a	Number of potential local MPPs in a PV array experiencing several irradiance levels.
n^i	Number of irradiance levels on the PV string i.
P_{mpj}^i	PV string i power at MPP_j^i.
R_s	Series resistance of the PV cell.
R_{sh}	Shunt resistance of the PV cell.
S_j^i	Sum of irradiance levels of all PV strings, except i, related to the operating currents at voltage V_{mpj}^i.
T_c	Operating temperature of a PV cell string.
V_{br}	Breakdown voltage of the PV cell.
V_{cell}	PV cell voltage.
V_{cs}	PV cell string voltage.
V_{mp},I_{mp}	PV module MPP voltage and current.
V_{mpj}^i	PV string i voltage at MPP_j^i.
V_{mpAj}^i	PV array voltage at $MPPA_j^i$.
V_{mpB}	PV array voltage at *MPPB*.
V_{oc}	PV module open circuit voltage.
V_{str}	PV string voltage.
β_{Vmp}	Temperature coefficient of V_{mp}.
β_{Voc}	Temperature coefficient of V_{oc}.
ΔV_D	Voltage drop on a conducting bypass diode.
κ_j^i	Voltage correlation coefficient of V_{mpAj}^i to V_{mpj}^i.
λ	Empirical coefficient for I_{mpj}^i.

Manuscript received May 15, 2014, revised Nov. 20, 2014, accepted Dec. 29, 2014. The work of Mr. G. N. Psarros was supported by the State Scholarships Foundation (IKY). Mr. E. Batzelis is supported in his PhD studies by "IKY Fellowships of Excellence for Postgraduate Studies in Greece - Siemens Program".

The authors are with the School of Electrical and Computer Engineering, National Technical University of Athens, Athens 15780, Greece (e-mail: gpsarros@mail.ntua.gr; batzelis@mail.ntua.gr; st@power.ece.ntua. gr).

I. INTRODUCTION

NON uniform illumination significantly affects the operation of photovoltaic (PV) generators, giving rise to multiple local maximum power points (MPPs), thus reducing the MPP tracking algorithm effectiveness [1]-[3] and system performance [4]. In [5], it is shown that two local maximum power points (MPPs) appear on the *P-V* curve of PV modules, operating under two irradiance levels. Other studies examine the electrical response of PV strings under partial shading conditions, reaching the conclusion that multiple MPPs are presented in the general case [5]-[11]. The importance of multiple MPPs on energy yield calculation is highlighted in [9]. In [10], the correlation between the number of local MPPs and the parameters of the PV modules in a partially shaded PV string is investigated, concluding that one or two MPPs are presented when two irradiance levels are considered. A complete shading analysis for the PV string is presented in [8], characterizing and identifying any number of MPPs in the general case of multiple irradiance levels. Moreover, in [11] arrays consisting of parallel connected short-strings and series connected strings are examined in terms of energy

yield, concluding that strings connected in series operate less efficiently under partial shading conditions.

In order to study the operation of a PV array under partial shading conditions and investigate the local MPPs, a suitable simulation model needs to be adopted, such as the commonly used single-diode PV cell electrical equivalent [12]-[13], which is suitable for uniform operating conditions. Enhanced and more sophisticated methods are required to simulate the electrical response of PV arrays under partial shading, [7], [14]-[16], which are usually iterative algorithms, their main drawbacks being the computational complexity and convergence issues. These drawbacks may be circumvented by the explicit model proposed in [8], in which the PV string voltage is expressed as an explicit function of its current using the Lambert *W* function, dispensing with the need for an iterative solution.

To avoid constructing the entire *I-V* curve in order to identify the global MPP, simplified formulae have been proposed in the past, which directly evaluate the local and global MPPs. In [5], empirical expressions for the MPP voltage and power are developed for a partially shaded PV module, while in [8] this approach is extended to introduce semi-empirical formulae for the voltage, current and power of all local MPPs of a partially shaded PV string. Module datasheet information and empirical coefficients are utilized to derive a simple and sufficiently accurate MPP estimation for series connected PV structures (modules and strings).

Concerning multi-string arrays, in [17] and [18], simple, non-electrical models are proposed, which are empirical in nature and are mainly based on a simplified consideration of the shading phenomenon, demonstrating only moderate accuracy. In [19] more accurate expressions are developed, yet limited to one level of shade. Inter-row shading of PV arrays is examined in [20], leading to a simplified expression, while the same topic is further analyzed in [21]. However, these approaches do not determine the local MPPs in a quantitative manner. This aspect is studied in [22], where closed-form expressions of voltage, current and power are developed for local MPPs of a partially shaded PV array, which present acceptable accuracy, but may not keep up with the complexity of the developed phenomena. The expressions proposed in [22] are based on assumptions for the calculation of current and voltage at MPP, which introduce inaccuracies (overestimation of current and underestimation of voltage), as discussed in Section V. Further, these formulae employ empirical coefficients, derived experimentally for the study-case PV modules of the paper, which may not be suitable for other modules.

It is therefore apparent that the identification and quantification of the MPPs developed in multi-string arrays under partial shading is an issue still open to investigation. Consistent and accurate MPP expressions, with a general applicability, are still missing from literature.

In this paper, the response of a PV array operating under non-uniform irradiance conditions is examined and a thorough analysis of the local MPPs is performed, to shed more light on this mode of operation. The modeling basis for this analysis is the approach described in [8], modified for multi-string PV arrays and validated by measurements. Subsequently, simplified expressions are developed, which provide the voltage, power and current of all MPPs of a partially shaded PV array, operating under any temperature and irradiance levels, in a simple and direct manner, avoiding time-consuming modeling and simulations. The expressions introduced in the paper apply for the general case of multi-string arrays, rely only on module datasheet information and are suitable for any commercial crystalline PV module. Their accuracy is validated by simulation of numerous shading scenarios, as well as by experimental results obtained by outdoor measurements. Their utility includes PV energy yield estimation and array optimization applications, while they may also prove a valuable tool in the development of shade resistant MPPT algorithms.

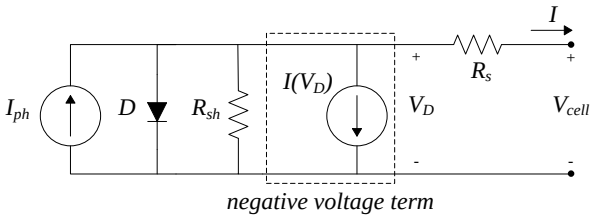

Fig. 1. PV cell electrical equivalent circuit.

This paper is structured as follows: In Section II the simulation model is described and experimentally validated. The model is utilized in Section III for the analysis of PV array shading. The results obtained are then employed in Section IV to derive simplified MPP expressions, which are validated in Section V by simulation and outdoor measurements.

II. PV Array Simulation Model

A. PV Cell Electrical Equivalent

A variety of PV cell electrical equivalent circuits are reported in the literature [4], [7]-[12], [14]-[16], [23]-[27], with the single-diode model being the most commonly used [7]-[12], [14]-[15], [23]-[24]. Although the double-diode model [14], [25] is more accurate under certain operating conditions, the single-diode equivalent combines simplicity with sufficient accuracy [24] and allows for the development of explicit models [8].

In this study, the electrical equivalent depicted in Fig. 1 is used. It is based on the single-diode model and properly expanded to represent accurately the negative diode breakdown operation [4], [16], [26]-[27]. The following equation applies:

$$I = I_{ph} - I_s\left(e^{\frac{V_{cell}+I\cdot R_s}{a}} - 1\right) - \frac{V_{cell}+I\cdot R_s}{R_{sh}} - \underbrace{b\left(V_{cell}+I\cdot R_s\right)\left(1-\frac{V_{cell}+I\cdot R_s}{V_{br}}\right)^{-m}}_{\text{term for negative breakdown voltage}} \quad (1)$$

where I_{ph}, I_s, a, R_s and R_{sh} are the 5 parameters of the model as described in [12] and b, V_{br}, m are coefficients related to negative voltage operation.

B. PV Array Modeling with the Lambert W Function

In order to reduce computational complexity and convergence issues related to the transcendental form of (1), eq. (1) is reformulated in [8] and expressed in the explicit form *V=f(I)* using the Lambert *W* function:

$$V_{cell}=\begin{cases} R_{sh}\left(I_{ph}+I_s\right)-\left(R_s+R_{sh}\right)\cdot I \\ -a\cdot W\left\{\dfrac{R_{sh}I_s}{a}\mathrm{e}^{\frac{R_{sh}\left(I_{ph}+I_s-I\right)}{a}}\right\}, \quad I\le I_{ph} \\ V_{br}-I\cdot R_s-z_{R\min} \quad , \quad I>I_{ph} \end{cases} \tag{2}$$

where $W\{x\}$ refers to the Lambert W function and $z_{R\min}$ to the minimum real root of the following equation, [8]:

$$\frac{1}{R_{sh}}\cdot z^4+\left(I_{ph}-I-\frac{V_{br}}{R_{sh}}\right)\cdot z^3+bV_{br}{}^3\cdot z-bV_{br}{}^4=0 \tag{3}$$

A group of series connected PV cells having a bypass diode connected in parallel is denoted as a cell string. The existence of bypass diodes is necessary to prevent hot-spot phenomena due to reversed operation of shaded cells under non-uniform illumination conditions. At negative voltages, the bypass diode conducts and the cell string voltage is thus limited to a typical value of -1V, depending on the diode characteristics. Eq. (4) gives the cell string voltage V_{cs} in an explicit form, assuming a number of N_s cells connected in series.

$$V_{cs}=\begin{cases} \sum_{i=1}^{N_s}V_{cell-i}(I) & ,I\le I_{SC,cs} \\ -a_{bp}\cdot\ln\left(\dfrac{I-I_{SC,cs}}{I_{sbp}}+1\right) & ,I>I_{SC,cs} \end{cases} \tag{4}$$

Assuming that each PV module is composed of N_{cs} cell strings and each PV string comprises N_m modules, the PV string voltage is expressed as:

$$V_{str}=\sum_{i=1}^{N_m\cdot N_{cs}}V_{cs-i}(I) \tag{5}$$

The model can be easily extended for the case of a PV array consisting of N_p strings, as reported in [8]. In order to determine the entire *I-V* curve of the array, (5) is used for each individual string and then curve superposition is applied using linear interpolation.

C. Experimental Validation

The modeling method described above is experimentally validated through outdoor measurements on a PV array comprising 2 strings connected in parallel, each consisting of 12 PV modules (datasheet characteristics shown in Table I). The physical layout of the examined PV array is depicted in Fig. 2. The five parameters of the model are calculated according to [12], whereas typical values for the negative voltage coefficients *b*, V_{br}, *m* are considered, [4], [16], [26], and bypass diode coefficients based on [15] and [16] are used.

In order to measure the PV array electrical response in partial shading conditions, various shade patterns were generated using a semitransparent fabric material with a transmission rate (*TR*) of 49%. The *I-V* characteristics of the array were measured using a variable resistor connected at the array terminals. For each pattern, the resistance was varied between minimum and maximum, changing the load applied to the PV array and thus the operating point on the I-V characteristic. During this procedure, the voltage and current was recorded using a portable DAQ measuring system and LabVIEW. The short circuit and open circuit points, in particular, were measured by shorting and open-circuiting the array terminals. The same procedure was applied for the experimental validation of Section V.

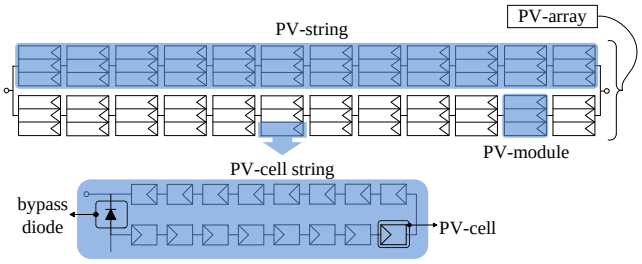

Fig. 2. Layout of the two-string PV array used in the measurements and its building blocks.

TABLE I
DATASHEET CHARACTERISTICS OF THE PV MODULES USED IN THE MEASUREMENTS (YINGLI YL-165)

Model	*Type*	N_s	N_{cs}	$I_{sc0}(A)$	$I_{mp0}(A)$	$V_{oc0}(V)$	$V_{mp0}(V)$
YL-165	mc-Si	16	3	7.2	7.9	29	23

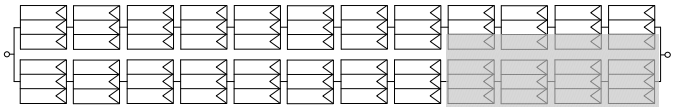

Fig. 3. Shading scenario with 4 and 12 shaded cell strings in each of the two PV strings (G=1.03 p.u., TR=49%, T_c=55°C).

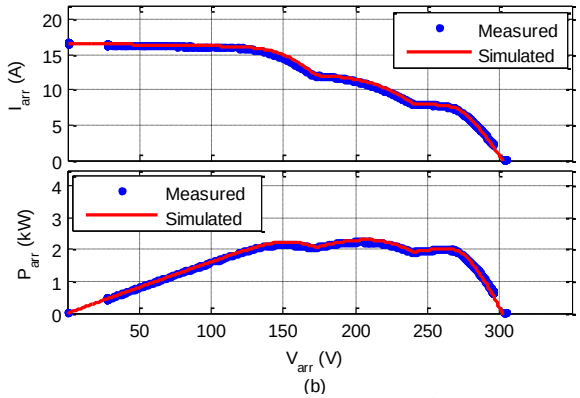

Fig. 4. Measured and simulated *I-V* and *P-V* curves of the shading scenario depicted in Fig.3.

An indicative shading scenario is depicted in Fig. 3 and the respective experimental and simulated *I-V* and *P-V* curves are illustrated in Fig. 4. The simulation results prove to be sufficiently accurate, a fact verified by additional measurements, as well as in [8].

III. PV ARRAY OPERATION UNDER PARTIAL SHADING

In this section, the operation of a partially shaded PV array is analyzed, leading to a systematic characterization of the developed local MPPs. What matters in this process is the extent of shade, in terms of the number of affected cell strings per PV string, whereas the exact location of the shaded modules within the array does not affect its electrical response [8].

A. PV String Operation under Partial Shading

A PV string illuminated at *n* irradiance levels G_j, j=1…n, sorted in decreasing order (G_j>G_{j+1}), develops up to *n* local MPPs [8]. At the same time, *n* groups of uniformly illuminated cell strings exist, each comprising N_j cell strings that operate at the same irradiance level G_j (j=1…n).

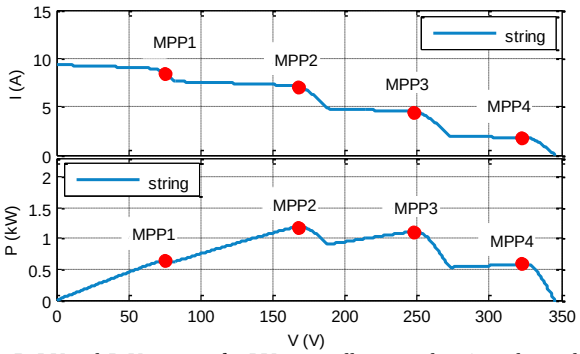

Fig. 5. *I-V* and *P-V* curves of a PV string illuminated at 4 irradiance levels (G_1=1.20, G_2=0.96, G_3=0.60, G_4=0.24 p.u. / T_c=25°C).

Referring to a specific MPP_j, cell string groups 1 to j operate at the current corresponding to the irradiance level G_j, while the remaining groups (j+1 to n) are bypassed by their conducting bypass diodes. An indicative scenario of a PV string illuminated at 4 irradiance levels is shown in Fig. 5, giving rise to 4 distinct MPPs.

B. Characterization of MPPs Appearing in a Partially Shaded PV Array

Explaining the response of a partially shaded PV array may be quite complicated, particularly when attempting to estimate the number of local MPPs that may appear on the *P-V* curve and identify the origin of each one of them.

The definitions given in Section III.A for the single PV string are extended to the PV array level. Each of the N_p parallel connected strings is illuminated at a number of n^i (i=1…N_p) irradiance levels G_j^i, j=1…n^i, sorted in decreasing order ($G_j^i > G_{j+1}^i$), that give rise to a maximum of n^i local MPPs on the *P-V* curve of the particular string. The notation MPP_j^i is used for these MPPs, where the superscript i denotes the examined string i and the subscript j the irradiance level G_j^i. The number of cell strings in each group, which experience the same irradiance level G_j^i, is denoted as N_j^i. In the following, superscript i and subscript j always refer to the string and irradiance level, respectively.

To facilitate understanding, the simple shading scenario of Fig. 3 is examined. The *I-V* curves of the two component strings and the characteristic of the entire array are depicted in Fig. 6, for operation at irradiance levels of 1 p.u. and 0.5 p.u., at 25°C. In Fig. 6, string 1 (red line) experiences two irradiance levels, G_1^1=1.0 p.u. and G_2^1=0.5 p.u., forming two groups of N_1^1=24 and N_2^1=12 cell strings respectively, leading to the appearance of two local maxima MPP_1^1 and MPP_2^1. Similarly for string 2 (green line), N_1^2=32 cell strings are illuminated at G_1^2=1.0 p.u. and N_2^2=4 shaded cell strings at G_2^2=0.5 p.u., giving rise to MPP_1^2 and MPP_2^2.

The resulting *I-V* curve of the entire array (blue line) exhibits 3 local MPPs in total, while a closer inspection reveals a correlation between those and the MPPs of the individual strings. Specifically, the array MPP at the highest current and the lowest voltage ($MPPA_1^1$) is closely related to the MPP_1^1 of string 1, because the shape of the array *I-V* characteristic in this region is dictated by the *I-V* curve of string 1, since the characteristic of string 2 is practically flat. Hence, the voltage at $MPPA_1^1$ is very close to the voltage V_{mp1}^1 of MPP_1^1 (slightly higher – zoom box in Fig. 6), while the array current is approximately twice the current I_{mp1}^1 of MPP_1^1 (the sum of I_{mp1}^1 and the current of string 2 at voltage V_{mp1}^1). Similarly, $MPPA_1^2$ of the array is closely related to MPP_1^2 of string 2, appearing at a voltage only slightly higher than V_{mp1}^2.

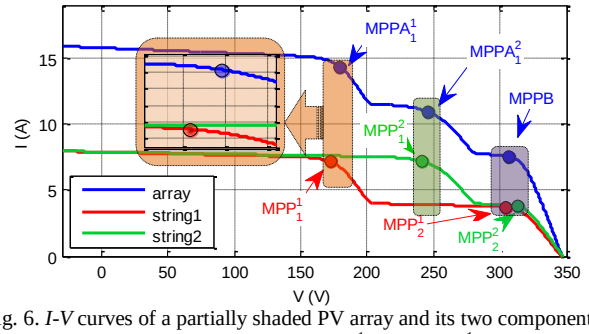

Fig. 6. *I-V* curves of a partially shaded PV array and its two component strings, for the shading scenario of Fig. 3 (G_1^1=1.0 p.u., G_2^1=0.5 p.u.).

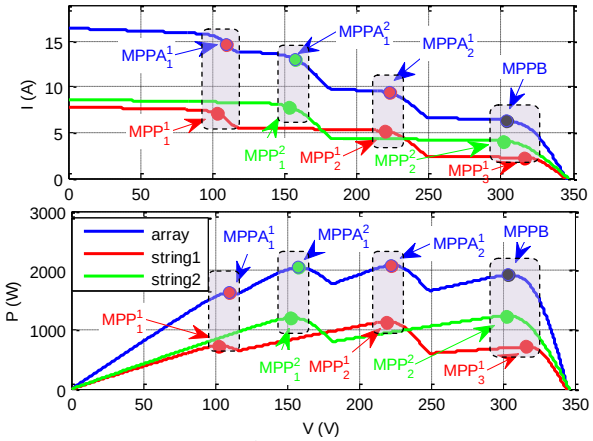

Fig. 7. *I-V* and *P-V* curves of a partially shaded PV array presenting 3 MPPAs and one MPPB.

Although the first two MPPs of the array are related to a specific MPP of one string, the last MPP of the array (*MPPB*) does not follow the same trend, but it comes from the interaction between the two last MPPs of the individual strings (MPP_2^1 and MPP_2^2). When a PV string operates at the rightmost MPP_{ni}^i, all cells in string i operate at the lowest current imposed by the most shaded cell string group, since all bypass diodes are reverse biased. In this case for the array, the voltages of the different MPP_{ni}^i of individual strings are very close to each other, regardless of the specific shading pattern of each string [8], leading to a single MPP for the entire array, as in Fig. 6.

Therefore, two types of array MPPs may be identified: One that is related to a specific string MPP_j^i (belonging in the first n^i-1 MPPs of string i) and denoted as $MPPA_j^i$, where i corresponds to string i and j to the irradiance level G_j^i on string i. The other type comprises a single MPP, denoted as *MPPB*, resulting from the interaction of the rightmost MPPs (MPP_{ni}^i) of all strings. Based on this characterization, the number of local MPPs for a partially shaded array is:

$$n_a = \sum_{i=1}^{N_p}\left(n^i - 1\right) + 1 = \sum_{i=1}^{N_p} n^i - N_p + 1 \qquad (6)$$

comprising n^i-1 MPPAs for each of the N_p strings of the array and a single *MPPB*. Notably, this is the maximum number of MPPs that may be observed, while the actual number may be smaller depending on the shading scenario.

In Fig. 7, another scenario of a 2-string array is illustrated to further clarify the previous analysis. String 1 is illuminated at three different irradiance levels (G_1^1=1.0 p.u, G_2^1=0.7 p.u. and G_3^1=0.3 p.u., with N_1^1=16, N_2^1=12 and N_3^1=8 cell strings respectively), while string 2 experiences two irradiance levels (G_1^2=1.1 p.u and G_2^2=0.55 p.u., with N_1^2=22 and N_2^2=14 cell strings). According to (6), up to four local MPPs may appear in the *P-V* curve of the array. $MPPA_1^1$, $MPPA_1^2$ and $MPPA_2^1$ are respectively related to MPP_1^1 of

string 1, MPP_1^2 of string 2 and MPP_2^1 of string 1. *MPPB* results from the interaction of MPP_3^1 and MPP_2^2, i.e. the last MPPs of each string.

The analysis presented in this section expands the concept introduced in [22], leading to clear characterization of the array MPPs. It is shown that the last MPP of the array (*MPPB*) differs from the others, while the number of potential local MPPs is not just the sum of the string MPPs, but it is determined according to (6).

IV. Derivation of Empirical Expressions for the MPPs of a Partially Shaded PV Array

In this section, simple explicit expressions are derived to calculate the voltage, current and power at each MPP of a partially shaded PV array, using only information provided in the datasheet of the PV modules. Similar expressions presented in [5] and [8] deal only with a PV module or string and they are only applicable at STC temperature (25°C). Nevertheless, the basis for the analysis at PV array level is provided by the expressions for MPP_j^i of a partially shaded PV-string, derived in [8]:

$$V_{mpj}^i = \sum_{g=1}^{j} N_g^i \left[\frac{G_j^i}{G_g^i} \frac{V_{mp0}}{N_{cs}} + \left(1 - \frac{G_j^i}{G_g^i}\right) \frac{V_{oc0}}{N_{cs}} \right] - \sum_{g=j+1}^{n_i} N_g^i \cdot \Delta V_D \quad (a)$$

$$I_{mpj}^i = G_j^i I_{mp0} \left[1 + \lambda \frac{\sum_{g=1}^{j-1} N_g^i}{N_m N_{cs}} \right] \quad (b) \quad (7)$$

$$P_{mpj}^i = V_{mpj}^i I_{mpj}^i \quad (c)$$

Expressions similar to (7) are used in [22], however the first term of (7a) is simplified and the effect of the extent of shading is ignored in (7b).

A. Formulae for $MPPA_j^i$

In order to derive the appropriate expressions for $MPPA_j^i$, its relation to MPP_j^i is taken into consideration.

1) Calculation of voltage V_{mpAj}^i:

As noted in Fig. 6 and 7, $MPPA_1^1$ appears at a slightly higher voltage than MPP_1^1 of string 1. To identify this offset, the simplified scenario of Fig. 8 is examined. String 2 is uniformly illuminated at G_1^2=1.0 p.u., while string 1 is shaded at a variable extent, from fully shaded to completely unshaded. The irradiance on the unshaded and shaded parts is G_1^1=1.0 p.u. and G_2^1=0.5 p.u. As the extent of shade changes, MPP_1^1, and hence $MPPA_1^1$, shift horizontally in a similar manner. The ratio V_{mpA1}^1/V_{mp1}^1 is illustrated in Fig. 9 as a function of the extent of the shade on string 1 (i.e. the fraction of the shaded cell strings N_2^1 to the number of total cell strings in the PV string). The calculation is repeated for 12 different PV modules. V_{mpA1}^1 is always higher than V_{mp1}^1, while their ratio remains constant at any shade extent higher than 15-20%. The difference between V_{mpA1}^1 and V_{mp1}^1 is close to 4% for all modules, leading to the adoption of the coefficient κ=0.04 as typical.

In Fig. 10, the mean ratio V_{mpA1}^1 to V_{mp1}^1 is plotted when the irradiance level G_1^2 on the unshaded string 2 varies from 0.5 p.u. to 1.0 p.u.. Apparently, the deviation between V_{mpA1}^1 and V_{mp1}^1 is affected by the operating current of string 2, which in turn is linearly related to the irradiance G_1^2. Hence the following approximation is introduced:

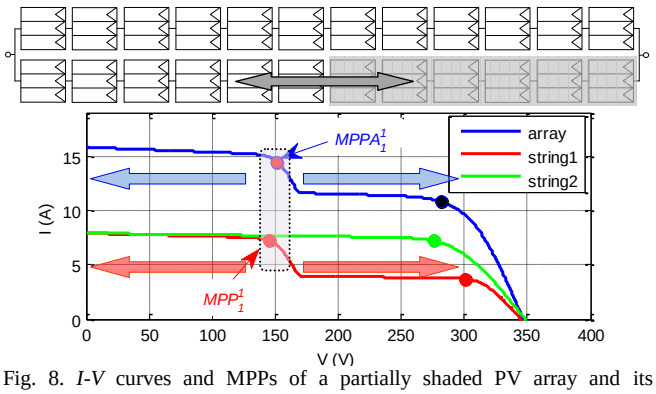

Fig. 8. *I-V* curves and MPPs of a partially shaded PV array and its component strings. String 2 remains unshaded, whereas string 1 is shaded at a variable extent.

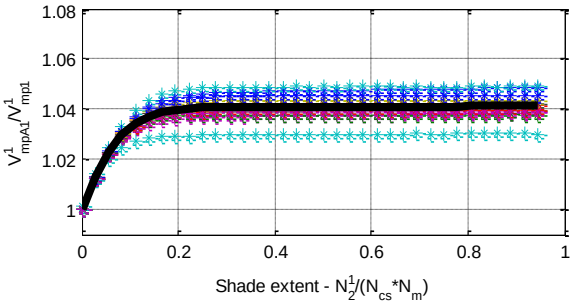

Fig. 9. Ratio V_{mpA1}^1 to V_{mp1}^1 as a function of the shade extent, for the scenarios of Fig.8. Ratio shown for 12 commercial PV modules and their mean value (solid line).

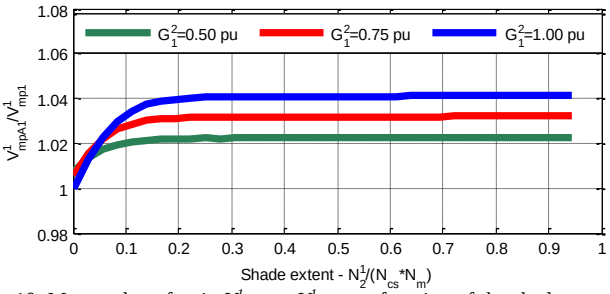

Fig. 10. Mean value of ratio V_{mpA1}^1 to V_{mp1}^1 as a function of the shade extent, for the scenarios of Fig. 8, assuming variable irradiance level on the unshaded part of the array. Same 12 commercial PV modules considered as in Fig. 9.

$$\frac{V_{mpA1}^1}{V_{mp1}^1} = 1 + \kappa \cdot G_1^2 \quad (8)$$

where κ=0.04 and V_{mp1}^1 is given by (7a) for ΔV_D=0.

If string 2 is not unshaded as considered above, but it is partially shaded at a smaller extent than string 1, as shown in Fig. 3, then (8) still applies, because the operating current of string 2 remains proportional to G_1^2, irrespectively of the multi-step shape of the *I-V* curve.

To extend (8) for multi-string PV arrays, the indicative case of Fig. 11 is considered, where the array consists of three PV strings, illuminated at different irradiance levels. Taking MPP_1^2 as an example, a similar analysis shows that the voltage offset between V_{mpA1}^2 and V_{mp1}^2 is linearly dependent on the operating currents of string 1 and string 3, and thus on the irradiance levels G_2^1 and G_1^3. The effect of each string is cumulative, leading to the expansion of (8):

$$\frac{V_{mpA1}^2}{V_{mp1}^2} = 1 + \kappa \cdot \left(G_2^1 + G_1^3\right) \quad (9)$$

Therefore, in the general case of multiple irradiance levels and a multi-string PV array, the voltage offset between $MPPA_j^i$ of the array and MPP_j^i of the respective

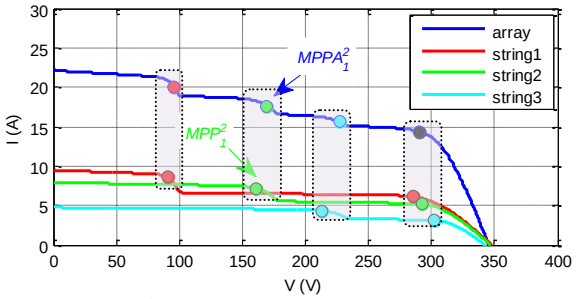

Fig. 11. *I-V* curves of a partially shaded PV array comprising three strings.

string is determined by the empirical coefficient κ and the sum S_j^i of the irradiance levels associated with the operating currents of all other strings except string i (i.e. strings 1, …, i-1, i+1,…, N_p) at the operating voltage V_{mpAj}^i:

$$\frac{V_{mpAj}^i}{V_{mpj}^i} = 1 + \kappa \cdot S_j^i \tag{10}$$

where

$$S_j^i = \sum_{\forall s \neq i} G_g^s \qquad \forall g : \sum_{r=1}^{j} N_r^i \in \left(\sum_{r=1}^{g-1} N_r^s, \sum_{r=1}^{g} N_r^s \right] \tag{11}$$

Concerning the empirical coefficient κ, a constant value of 0.04 is a good approximation when the shade extent is greater than 20%. Below this threshold, κ varies from 0 to 0.04 in a non-linear way (Fig. 9). If a better accuracy is sought, at the expense of simplicity, eq. (12) below can be used, which is accurate over the entire range of shade extent:

$$\kappa_j^i = 0.04 - 0.04 \cdot 10^{\left\{ -15 \cdot \frac{\min_{\forall s,g} \left\{ \sum N_g^s \middle| \sum N_g^s > \sum_{r=1}^{j} N_r^s \right\} - \sum_{r=1}^{j} N_r^s}{\sum_{g=1}^{j} N_g^i} \right\}} \tag{12}$$

To obtain the voltage V_{mpAj}^i of $MPPA_j^i$, (7a) is substituted in (10) and the following expression is derived when ΔV_D=0:

$$V_{mpAj}^i = \left(1 + \kappa_j^i S_j^i\right) \sum_{g=1}^{j} N_g^i \left[\frac{G_j^i}{G_g^i} \frac{V_{mp}}{N_{cs}} + \left(1 - \frac{G_j^i}{G_g^i}\right) \frac{V_{oc}}{N_{cs}} \right] \tag{13}$$

In the previous analysis, the voltage drop on the bypass diodes was neglected for simplicity (ΔV_D=0). If a non-zero voltage drop ΔV_D is considered, the complete equation for V_{mpAj}^i is obtained:

$$V_{mpAj}^i = \left(1 + \kappa_j^i S_j^i\right) \sum_{g=1}^{j} N_g^i \left[\frac{G_j^i}{G_g^i} \frac{V_{mp}}{N_{cs}} + \left(1 - \frac{G_j^i}{G_g^i}\right) \frac{V_{oc}}{N_{cs}} \right] - \sum_{g=j+1}^{n_i} N_g^i \cdot \Delta V_D \tag{14}$$

where S_j^i is given by (11), κ_j^i may be either considered constant at 0.04 or calculated from (12), and ΔV_D can be assumed nearly equal to 1V (or a more accurate value, if available).

2) Calculation of current I_{mpAj}^i:

Assuming again the shading scenarios of Fig. 8, the ratio I_{mpA1}^1 / I_{mp1}^1 is plotted in Fig. 12 against the extent of shade and in Fig. 13 against the level of irradiance on the unshaded string. It is observed that its average value remains practically constant as the shaded area varies (very close to 2 for G_1^2 =1.0 p.u.), while it changes proportionally with the irradiance G_1^2 on the unshaded string 2. This ratio obviously depends also on the irradiance G_1^1 on the shaded string 1,

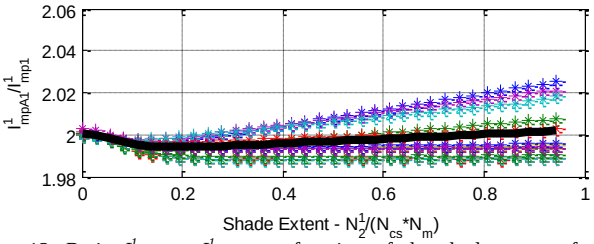

Fig. 12. Ratio I_{mpA1}^1 to I_{mp1}^1 as a function of the shade extent, for the scenarios of Fig.8. Ratio shown for 12 commercial PV modules and their mean value (solid line).

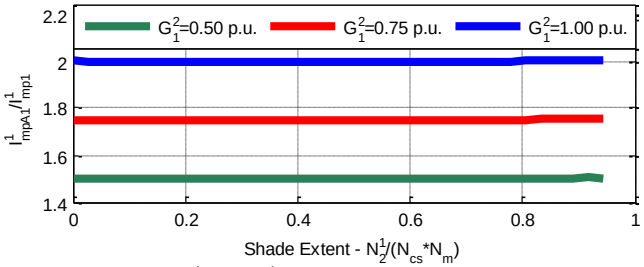

Fig. 13. Mean ratio I_{mpA1}^1 to I_{mp1}^1 for 12 commercial PV modules at the shading scenarios of Fig.8, with variable irradiance level on the unshaded string.

since it determines the current I_{mp1}^1 in a linear way. In fact, the ratio I_{mpA1}^1 to the nominal current I_{mp} may be simply approximated in all cases by the sum of the irradiance levels G_1^1 and G_1^2 (since I_{mp1}^1 is linearly dependent on the irradiance level G_1^1):

$$I_{mpA1}^1 \overset{Fig.13}{=} I_{mp1}^1 + G_1^2 I_{mp} \overset{I_{mp1}^1 = G_1^1 I_{mp}}{=} G_1^1 I_{mp} + G_1^2 I_{mp} \Rightarrow$$

$$\frac{I_{mpA1}^1}{I_{mp}} = G_1^1 + G_1^2 \tag{15}$$

Eq. (15) can be readily extended for the case of the multi-string PV array of Fig.11, by observing that the current I_{mpA1}^2 is linearly dependent on the operating currents of string 1, string 2 and string 3, and thus the respective irradiance levels G_2^1, G_1^2 and G_1^3:

$$\frac{I_{mpA1}^2}{I_{mp}} = G_1^2 + G_2^1 + G_1^3 \tag{16}$$

In the general case of multiple irradiance levels and a multi-string PV array, the following expression holds for I_{mpAj}^i:

$$I_{mpAj}^i = I_{mp} \cdot (G_j^i + S_j^i) \tag{17}$$

where S_j^i is given by (11), and the term included in the parenthesis corresponds to the sum of the appropriate irradiance levels of all strings (including the G_j^i of string i).

B. Formulae for MPPB

1) Calculation of Voltage V_{mpB}:

By observing the characteristics in Fig. 6-8 and Fig. 11, it is evident that *MPPB* always lies in the same interval as the voltages V_{mpni}^i of the rightmost MPPs of the strings, whose proximity leads to the formation of a single *MPPB* for the entire array. This proximity arises from the fact that, regardless of the shading pattern and intensity, at MPP_{ni}^i none of the cell strings is bypassed and their operating voltages deviate only slightly depending on their irradiance level [8]. This aspect is graphically demonstrated in Fig. 14, where the V_{mpni}^i variation with the extent and intensity of shade is shown to be limited.

Therefore, given the close proximity of voltages V_{mpni}^i and the unavailability of a reasonably complex analytical way to

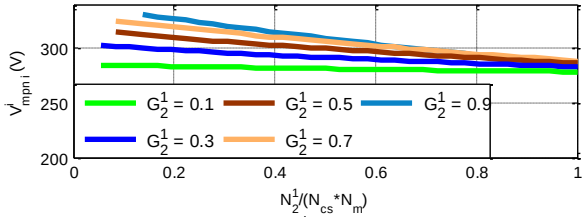

Fig. 14. Variation of the voltage V^i_{mpni} with the extent of the shade on a partially shaded PV string, at different intensities.

quantify the derivation of *MPPB* from the associated MPPs of the individual strings, its voltage V_{mpB} is simply approximated by the average value of the string MPP voltages V^i_{mpni}:

$$V_{mpB} = \frac{1}{N_p}\sum_{i=1}^{N_p} V^i_{mpn_i} \overset{(7a)}{=} \frac{1}{N_p}\sum_{i=1}^{N_p}\sum_{g=1}^{n_i} N^i_g \left[\frac{G^i_j}{G^i_g}\frac{V_{mp}}{N_{cs}} + \left(1-\frac{G^i_j}{G^i_g}\right)\frac{V_{oc}}{N_{cs}}\right] \quad (18)$$

2) Calculation of Current I_{mpB}:

Based on the previous analysis, I_{mpB} is given by the sum of the currents I^i_{mpni} of the component strings, derived from (7b):

$$I_{mpB} = I_{mp}\sum_{i=1}^{N_p}\left(G^i_{n_i}\left[1+\lambda\frac{\sum_{g=1}^{n_i-1} N^i_g}{N_m N_{cs}}\right]\right) \quad (19)$$

where λ is an empirical constant equal to 0.06 [8].

C. Temperature Effect

So far, expressions (14), (17), (18) and (19) provide the voltage and current of all MPPs of a partially shaded PV array, considering the multiple irradiance levels G^i_j on different parts of the array. To take into account the temperature effect, the following expressions can be used for the terms I_{mp}, V_{mp} and V_{oc}:

$$I_{mp} = I_{mp0} + \alpha_{I_{mp}}\left(T_C - T_0\right) \quad \text{(a)}$$
$$V_{mp} = V_{mp0} + \beta_{V_{mp}}\left(T_C - T_0\right) \quad \text{(b)} \quad (20)$$
$$V_{oc} = V_{oc0} + \beta_{V_{oc}}\left(T_C - T_0\right) \quad \text{(c)}$$

where α_{Imp}, β_{Vmp} and β_{Voc} are the temperature coefficients of the MPP current, the MPP voltage and the open circuit voltage, as given in the PV module datasheet, and T_0=25 °C is the temperature at STC. In the absence of specific values for α_{Imp} and β_{Vmp}, α_{Isc} (short circuit current temperature coefficient) and β_{Voc} can be used instead, as a reasonable approximation. In (20), a common temperature T_c can be assumed for all cells, while more refined approaches are possible if a suitable thermal model is available.

V. Validation of the MPP Expressions via Simulation and Experimental Results

The accuracy of the simplified formulae introduced in the previous section is validated first by simulation, employing the explicit PV array model described in Section II, and then by outdoor measurements on a real PV array.

A. Simulation Results

In the simulation process, a three-string PV array is considered, comprising 12 modules per string, whose characteristics are given in Table I (Yingli Yl-165). The array experiences six different irradiance levels, varying in the range of 100 W/m^2 to 1200 W/m^2, and three different operating temperatures, 25° C, 45° C and 65° C, leading to a total number of 190,515 scenarios.

TABLE II
MPP Estimation Error of the Proposed Formulae for a Partially Shaded Three-String PV Array

	Error %					
MPPs	*Current*		*Voltage*		*Power*	
	Rms	*Max*	***Rms***	*Max*	***Rms***	*Max*
$MPPA^1_1$	**2.43**	11.40	**2.29**	9.03	**2.84**	12.25
$MPPA^1_2$	**3.17**	11.01	**1.98**	8.69	**2.92**	15.05
$MPPA^2_1$	**1.77**	11.85	**2.36**	8.94	**2.42**	14.56
$MPPA^3_1$	**1.70**	9.84	**2.67**	8.22	**2.08**	4.89
$MPPA^3_2$	**3.20**	8.08	**2.59**	8.67	**3.87**	10.52
MPPB	**0.57**	3.71	**2.08**	7.56	**2.20**	9.02

TABLE III
MPP Estimation Error Using the Formulae of [22], for the same Partially Shaded Three-String PV Array as in Table II

	Error %					
MPPs	*Current*		*Voltage*		*Power*	
	Rms	*Max*	***Rms***	*Max*	***Rms***	*Max*
$MPPA^1_1$	**3.43**	28.50	**2.99**	14.31	**1.57**	23.14
$MPPA^1_2$	**17.18**	64.90	**9.89**	39.31	**14.99**	62.14
$MPPA^2_1$	**4.43**	94.59	**4.06**	16.76	**3.62**	82.98
$MPPA^3_1$	**3.02**	42.35	**4.07**	14.53	**2.36**	34.93
$MPPA^3_2$	**21.50**	74.91	**8.69**	23.24	**18.81**	73.33
MPPB	**0.94**	15.92	**3.01**	16.98	**2.55**	14.06

Estimation errors of (14), (17), (18) and (19) for all MPPs on the array characteristic are shown in Table II, evaluated against the results of the detailed model of Section II, which is used to simulate the entire *I-V* curve for each shading scenario and identify all local MPPs. The rms error of the simplified equations is very low, not exceeding 4%, while maximum errors up to 15% are observed. The latter correspond to minor local MPPs appearing under extreme shading scenarios, which are not important, as their actual power is very small and they never constitute the global MPP of the array.

Another important aspect of the proposed simplified expressions is their computational efficiency. Simulation of the 190,515 shading scenarios of Table II required only 20 min, as compared to almost 10 days using the detailed model of Section II.

For comparison purposes, the formulae proposed in [22] are also evaluated for the same scenarios and MPP estimation errors are presented in Table III. The model of [22] employs empirical expressions to extrapolate V_{mp}, I_{mp}, V_{oc} and I_{sc} from STC to the actual irradiance and temperature; such expressions are derived by measurements on the specific PV module used and cannot be generalized. Since such relations are not available for the study-case module (Yingli Yl-165), a proportional dependence of currents on irradiance and voltages on temperature is assumed, as expressed in (20). Further, the model of [22] calculates multiple maxima in the vicinity of the rightmost MPP, rather than a unique *MPPB*. Here, the MPP with the highest power is selected as MPPB among them and used in the comparison.

Comparing Tables II and III, the formulae introduced in this paper appear to be considerably more accurate. This is mainly due to the underestimation of voltage (V^i_{mpAj} is assumed equal to V^i_{mpj}) and overestimation of current (I^i_{mpAj} is assumed to be 5% higher than I^i_{mpj}) in the model of [22]. Nevertheless, it is noted that the largest errors in Table III occur at minor (low power) MPPs, developing under unrealistic operating conditions.

As a further validation of the proposed formulae, different commercially available PV modules are considered and the shading scenarios analysis is repeated for the same three-string array configuration. Using the detailed model of Section II, the entire *P-V* characteristic is determined for each of the 190,515 shading patterns. The operating point with the highest power is taken as the reference GMPP for each scenario, to evaluate the accuracy of the maximum local MPP estimate of the proposed expressions. The resulting deviations are given in Table IV, presenting rms and maximum errors below 3% and 15% respectively.

B. Experimental Results

For the experimental validation of the proposed equations, measurements on an operating PV array are conducted using the procedure described in Section II.C. The examined PV array comprises 2 strings connected in parallel, each consisting of 12 Yingli Yl-165 PV modules connected in series. Several shading patterns are generated using a semitransparent fabric with a transmission rate of 49%, while the *I-V* curves are measured using a variable resistor connected to the array terminals, as explained in Section II.C.

The incident irradiance level (G_1^1, G_1^2 on the unshaded part and G_2^1, G_2^2 on the shaded part), PV module operating temperature and shade extent are recorded for each scenario and illustrated in Table V. The local MPPs are identified from the measured *I-V* and *P-V* curves for each case. Thereafter, (14), (17), (18) and (19) are applied to evaluate the voltage, current and power at each MPPs, which are then compared to the measured values. The respective errors are summarized in Table VI. It is clear that the performance of the proposed simplified expressions is quite satisfactory in real world conditions, presenting errors lower than 5% in all scenarios.

TABLE IV
GLOBAL MPP ESTIMATION ERRORS OF THE PROPOSED FORMULAE, APPLIED TO A PARTIALLY SHADED THREE-STRING PV ARRAY, ASSUMING DIFFERENT COMMERCIAL PV MODULES

Error % at Global MPP						
PV module	*Current*		*Voltage*		*Power*	
	Rms	*Max*	***Rms***	*Max*	***Rms***	*Max*
Siliken SLK60P6L	**1.91**	7.49	**2.05**	8.62	**2.74**	14.61
Bosch M60-245	**1.86**	5.23	**2.16**	8.70	**2.84**	12.25
Upsolar UP-M240P	**1.85**	7.37	**2.03**	8.65	**2.71**	13.73
SCHOTT Perform 240	**2.03**	7.19	**1.93**	8.60	**2.76**	12.89
Suntech STP 280	**1.98**	7.51	**2.46**	8.68	**2.98**	13.36

TABLE V
EXPERIMENTAL VALIDATION SCENARIOS (PV ARRAY SHOWN IN FIG. 2)

Scenario	N_1^1	N_2^1	N_1^2	N_2^2	G_1^1,G_1^2	G_2^1,G_2^2	T_c (°C)
1	30	6	34	2	0.990	0.485	53
2	24	12	32	4	1.030	0.505	57
3	12	24	28	8	1.090	0.534	55
4	6	30	26	10	1.050	0.515	54
5	21	15	26	10	1.038	0.509	55
6	33	3	33	3	0.981	0.481	54
7	21	15	21	15	1.050	0.515	58

TABLE VI
MPP EVALUATION ERRORS USING THE SIMPLIFIED EXPRESSIONS OF SECTION IV, FOR THE SCENARIOS OF TABLE V

Error %									
Scenario	$MPPA_1^1$			$MPPA_1^2$			*MPPB*		
	P	*I*	*V*	*P*	*I*	*V*	*P*	*I*	*V*
1	0.8	1.0	0.6	---	---	---	1.8	1.0	0.8
2	0.1	2.1	2.0	0.1	0.9	1.0	0.4	0.1	0.5
3	0.5	4.6	4.9	0.8	1.3	0.5	0.5	1.1	0.6
4	---	---	---	1.0	1.9	0.9	0.5	1.7	1.1
5	0.6	2.5	1.8	0.2	0.9	1.1	0.1	0.3	0.4
6	1.5	1.4	0.1	---	---	---	1.9	0.4	1.5
7	2.6	1.7	1.0	---	---	---	0.1	0.2	0.3

VI. CONCLUSION

In this paper, the electrical response of partially shaded PV arrays, comprising several parallel-connected strings, is investigated. Under non-uniform illumination conditions, a PV array presents several local MPPs, which are shown to be closely related to the MPPs of the individual strings. Based on this observation, the maximum number of array MPPs is determined and the MPPs are characterized in terms of their voltage and current.

Subsequently, simplified equations are derived to evaluate the voltage, current and power of all MPPs of a PV array operating under non-uniform illumination conditions, in a direct and straightforward manner, using only basic datasheet information. The proposed formulae are validated by simulation and via outdoor measurements. Due to their accuracy, simplicity, computational efficiency and generic formulation, the simplified equations are suitable for fast energy yield calculations in shaded PV arrays.

VII. REFERENCES

[1] H. Patel and V. Agarwal, "Maximum power point tracking scheme for PV systems operating under partially shaded conditions," *IEEE Trans. Ind. Electron.*, vol. 55, no.4, pp. 1689-1698, Apr. 2008.

[2] N. Femia, G. Lisi, G. Petrone, G. Spagnuolo and M. Vitelli, "Distributed maximum power point tracking of photovoltaic arrays: Novel approach and system analysis," *IEEE Trans. Ind. Electron.*, vol. 55, no.7, pp. 2610-2621, Jul. 2008.

[3] K. Ishaque and Z. Salam, "A deterministic particle swarm optimization maximum power point tracker for photovoltaic system under partial shading condition," *IEEE Trans. Ind. Electron.*, vol. 60, no.8, pp. 3195-3206, Aug. 2013.

[4] S. Silvestre and A. Chouder, "Effects of shadowing on photovoltaic module performance," *Prog. Photovolt.: Res. Appl.*, vol. 16, no.2, pp. 141-149, Mar. 2008.

[5] E. Paraskevadaki and S. Papathanassiou, "Evaluation of MPP voltage and power of mc-Si PV modules in partial shading conditions," *IEEE Trans. Energy Convers.*, vol. 26, no. 3, pp. 923–932, Sep. 2011.

[6] M.F.N. Tajuddin, S.M. Ayob, and Z. Salam, "Tracking of maximum power point in partial shading condition using differential evolution (DE)," in *Proc. PECon 2012*, Kota Kinabalu, Malaysia, Dec. 2012, pp. 384-389.

[7] H. Patel and V. Agarwal, "MATLAB-based modeling to study the effects of partial shading on PV array characteristics," *IEEE Trans. Energy Convers.*, vol. 23, no. 1, pp. 302–310, Mar. 2008.

[8] E. Batzelis, I. Routsolias, and S. Papathanassiou, "An explicit PV string model based on the Lambert W function and simplified MPP expressions for operation under partial shading," *IEEE Trans. Sustain. Energy*, vol. 5, no. 1, pp. 301–312, Jan. 2014.

[9] A. Maki, S. Valkealahti, and J. Leppaaho, "Operation of series-connected silicon-based photovoltaic modules under partial shading conditions," *Prog. Photovolt.: Res. Appl.*, vol. 20, no.3, pp. 298-309, May 2012.

[10] A. Maki and S. Valkealahti, "Effect of photovoltaic generator components on the number of MPPs under partial shading conditions," *IEEE Trans. Energy Convers.*, vol. 28, no. 4, pp. 1008–1017, Dec. 2013.

[11] A. Maki and S. Valkealahti, "Power losses in long string and parallel-connected short strings of series-connected silicon-based photovoltaic modules due to partial shading conditions," *IEEE Trans. Energy Convers.*, vol. 27, no.1, pp. 173-183, Mar. 2012.

[12] W. De Soto, S.A. Klein, and W.A. Beckman, "Improvement and validation of a model for photovoltaic array performance," *Sol. Energy*, vol. 80, no.1, pp. 78-88, Jan. 2006.

[13] H. Tian, F. Mancilla-David, K. Ellis, E. Muljadi, and P. Jenkins, "A cell to-module-to-array detailed model for photovoltaic panels," *Sol. Energy*, vol. 88, no.9, pp. 2695-2706, Sep. 2012.

[14] V. Quaschning and R. Hanitsch, "Numerical simulation of current voltage characteristics of photovoltaic systems with shaded solar cells," *Sol. Energy*, vol. 56, no. 6, pp.513-520, Jun. 1996.

[15] E. Karatepe, M. Boztepe, and M. Colak, "Development of a suitable model for characterizing photovoltaic arrays with shaded solar cells," *Sol. Energy*, vol. 81, no.8, pp. 977-992, 2007.
[16] G. Liu, S. K. Nguang, and A. Partridge, "A general modeling method for I-V characteristics of geometrically and electrically configured photovoltaic arrays," *Energ. Convers. Manage.*, vol. 52, no.12, pp. 3439-3445, Nov. 2011.
[17] F. Martinez-Moreno, J. Munoz, and E. Lorenzo, "Experimental model to estimate shading losses on PV arrays," *Sol. Energy Mater. Sol. Cells*, vol. 94, no.12, pp. 2298–2303, Dec. 2010.
[18] N. Thakkar, D. Cormode, V. Lonij, S. Pulver, and A. Cronin, "A simple non-linear model for the effect of partial shade on PV systems," in *Proc. 35th PVSC 2010*, Honolulu, HI, United States, Jun. 2010, pp. 2321–2326.
[19] P. Rodrigo, E. F. Fernández, F. Almonacid, and P.J. Pérez-Higueras, "A simple accurate model for the calculation of shading power losses in photovoltaic generators," *Sol. Energy*, vol. 93, pp. 322-333, Jul. 2013.
[20] K. Brecl and M. Topic, "Self-shading losses of fixed free-standing PV arrays," *Renew. Energ.*, vol. 36, no. 11, pp. 3211-3216, Nov. 2011.
[21] C. Deline, A. Dobos, S. Janzou, J. Meydbray, and M. Donovan, "A simplified model of uniform shading in large photovoltaic arrays," *Sol. Energy*, vol. 96, pp. 274-282, Oct. 2013.
[22] S. Moballegh ang J. Jiang, "Modeling, prediction, and experimental validations of power peaks of PV arrays under partial shading conditions," *IEEE Trans. Energy Convers.*, vol. 5, no. 1, pp. 293-300, Jan. 2014.
[23] D. D. Nguyen and B. Lehman, "Modeling and simulation of solar PV arrays under changing illumination conditions," in *Proc. 2006 IEEE COMPEL Workshop, Rensselaer Polytechnic Institute*, Troy, NY, USA, Jul. 2006, pp. 295–299.
[24] M. G. Villalva, J. R. Gazoli, and E. R. Filho, "Comprehensive approach to modeling and simulation of photovoltaic arrays," *IEEE Trans. Power Electron.* vol. 24, no.5, pp. 1198-1208, May 2009.
[25] Z. Salam, K. Ishaque, and H. Taheri, "An improved two-diode photovoltaic (PV) model for PV system," in *Proc. PEDES 2010 & 2010 Power India*, New Delhi, India, pp. 1–5, Dec. 2010.
[26] H. Kawamura, K. Naka, N. Yonekura, S. Yamanaka, H. Kawamura, H. Ohno, and K. Naito, "Simulation of characteristics of a PV module with shaded PV cells," *Sol. Energy Mater. Sol. Cells*, vol. 75, no.3-4, pp. 613–621, Feb. 2003.
[27] J. W. Bishop, "Computer simulation of the effects of electrical mismatches in photovoltaic cell interconnection circuits," *Sol. Cells*, vol. 25, no.1, pp. 73–89, 1988.

VIII. BIOGRAPHIES

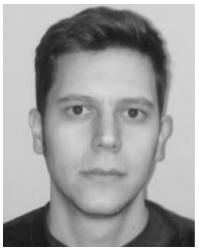

Georgios N. Psarros (S'14) received the Diploma in Electrical & Computer Engineering, in 2010, and his M.Sc. degree on Energy Production & Management, in 2014, both from the National Technical University of Athens (NTUA), Greece, where he is currently working towards the Ph.D. degree.

His research interests lie in the field of renewable energy sources, especially on photovoltaic technology and energy management of non-interconnected island grids.

Efstratios I. Batzelis (S'14) received the Diploma in Electronic & Computer Engineering from the Technical University of Crete (TUC), Chania, Greece, in 2009, and his M.Sc. degree on Energy Production & Management from the National Technical University of Athens (NTUA), Athens, Greece, in 2012, where he is currently working towards the Ph.D. degree.

His current research interests include renewable energy technologies, especially photovoltaic system design and simulation under mismatched operation.

Stavros A. Papathanassiou (S'93–M'98–SM'10) received the Diploma degree in Electrical Engineering and the Ph.D. degree from the National Technical University of Athens (NTUA), Athens, Greece, in 1991 and 1997, respectively.

He was with the Distribution Division of the Public Power Corporation of Greece, engaged in power quality and DG studies. In 2002, he joined the Electric Power Division of NTUA, where he is currently an Associate Professor. His research interests are in the field of RES and DG, including wind turbine and PV technology, storage applications and integration of DG to the grid. In 2009-2012 he was a Member of the Board of the Hellenic Transmission System Operator.